Geomicrobiology Journal
Publication details, including instructions for authors and subscription information:
http://www.tandfonline.com/loi/ugmb20

Lipid and DNA Evidence of Dominance of Planktonic Archaea Preserved in Sediments of the South China Sea: Insight for Application of the TEX_{86} Proxy in an Unstable Marine Sediment Environment

Yuli Wei [a b], Peng Wang [a], Meixun Zhao [a c], Xuejie Li [d], Hongfeng Lu [d] & Chuanlun L. Zhang [a b]

[a] State Key Laboratory of Marine Geology, Tongji University, Shanghai, China
[b] Department of Marine Sciences, University of Georgia, Athens, Georgia, USA
[c] Key Laboratory of Marine Chemistry Theory and Technology, Ocean University of China, Qingdao, China
[d] Institute of Marine Environmental and Engineering Geology, Guangzhou Marine Geological Survey, Guangzhou, China

Accepted author version posted online: 03 Oct 2013.Published online: 24 Feb 2014.

To cite this article: Yuli Wei, Peng Wang, Meixun Zhao, Xuejie Li, Hongfeng Lu & Chuanlun L. Zhang (2014) Lipid and DNA Evidence of Dominance of Planktonic Archaea Preserved in Sediments of the South China Sea: Insight for Application of the TEX_{86} Proxy in an Unstable Marine Sediment Environment, Geomicrobiology Journal, 31:4, 360-369, DOI: 10.1080/01490451.2013.824051

To link to this article: http://dx.doi.org/10.1080/01490451.2013.824051

Geomicrobiology Journal (2014) **31**, 360–369

ISSN: 0149-0451 print / 1521-0529 online
DOI: 10.1080/01490451.2013.824051

Taylor & Francis
Taylor & Francis Group

Lipid and DNA Evidence of Dominance of Planktonic Archaea Preserved in Sediments of the South China Sea: Insight for Application of the TEX_{86} Proxy in an Unstable Marine Sediment Environment

YULI WEI[1,2], PENG WANG[1], MEIXUN ZHAO[1,3*], XUEJIE LI[4], HONGFENG LU[4], and CHUANLUN L. ZHANG[1,2*]

[1]*State Key Laboratory of Marine Geology, Tongji University, Shanghai, China*
[2]*Department of Marine Sciences, University of Georgia, Athens, Georgia, USA*
[3]*Key Laboratory of Marine Chemistry Theory and Technology, Ocean University of China, Qingdao, China*
[4]*Institute of Marine Environmental and Engineering Geology, Guangzhou Marine Geological Survey, Guangzhou, China*

Received June 2013, Accepted July 2013

The marine planktonic archaea are dominated by Thaumarchaeotal Marine Group I, which is characterized by the lipid biomarker thaumarchaeol. The marine benthic archaea are characterized by greater diversity of currently unknown species whose lipid biomarker signatures are uncertain. In this study, a sediment core from the northwestern part of the South China Sea (SCS) (water depth 1474 m) was analyzed using molecular DNA and lipid biomarker approaches. While 16S rRNA gene analysis showed changing archaeal community structures with sediment depth, this change had little impact on the fossil record of archaeal lipids that are characteristic of the planktonic community. As a result, the fossil archaeal lipids recorded paleo sea surface temperature of the SCS since the last glacial maxima by the TEX_{86} proxy, which agreed generally with the winter temperature recorded by planktonic foraminiferas collected from the same area of the SCS that hosted mass-transported deposits. This suggests that this deep water deposit may have partially preserved paleoclimate record reflecting seasonal temperature variation in a near shore setting, which is in contrast to annual sea surface temperature or sub sea surface temperature variation recorded by TEX_{86} in the open ocean.

Keywords: mass-transported deposits, paleotemperature, planktonic archaea, South China Sea, TEX_{86}, thaumarchaeol, thaumarchaeota

Introduction

Archaea are ubiquitous in the environment and play an important role in the global carbon and nitrogen cycle (Schleper et al. 2005). They biosynthesize isoprenoid glycerol dialkyl glycerol tetraethers (GDGTs) as major membrane lipids, which include a series of compounds with zero to four cyclopentyl moieties (Figure 1) (Schouten et al. 2002). In Thaumarchaeota a cyclohexyl moiety also exists along with other four cyclepentyl rings, which makes the compound a special name called thaumarchaeol, previously known as crenarchaeol (Figure 1) (Schouten et al. 2000; Sinninghe Damsté et al. 2002). Culture experiments show that the distribution of isoprenoid GDGTs with cyclopentyl moieties increases with temperature (Boyd et al. 2011; Lai et al. 2008; Uda et al. 2001). Schouten et al. (2002) introduced the TEX_{86} index (tetraether index of tetraethers consisting of 86 carbons) as a sea surface temperature (SST) proxy based on the relative abundance of isoprenoid GDGTs, which has been widely used but many questions remain in terms of the climate interpretations of the TEX_{86} temperature records (Jia et al. 2012; Schouten et al. 2007; Schouten et al. 2013; Wei et al. 2011).

For example, Kim et al. (2008) showed that TEX_{86} values corresponded well with annual mean temperature of upper mixed layer of the ocean on the basis of analysis of 287 global core–top sediments; other studies have shown that TEX_{86} reflected the temperature of a particular season of the year (Castaneda et al. 2010; Herfort et al. 2006; Huguet et al. 2011; Leider et al. 2010) and TEX_{86} also may have corresponded to subsurface temperature better than SST (Jia et al. 2012; Li et al. 2013; Wuchter et al. 2006; Yamamoto et al. 2012).

GDGT distributions in the ocean can be affected by lateral transport of isoprenoid GDGTs (Kim et al. 2009; Shah et al.

*Address correspondence to Meixun Zhao or Chuanlun L. Zhang, State Key Laboratory of Marine Geology, Tongji University, Shanghai 200092, China; Email: maxzhao04@yahoo.com or Archaea.zhang@gmail.com
Color versions of one or more of the figures in the article can be found online at www.tandfonline.com/ugmb.

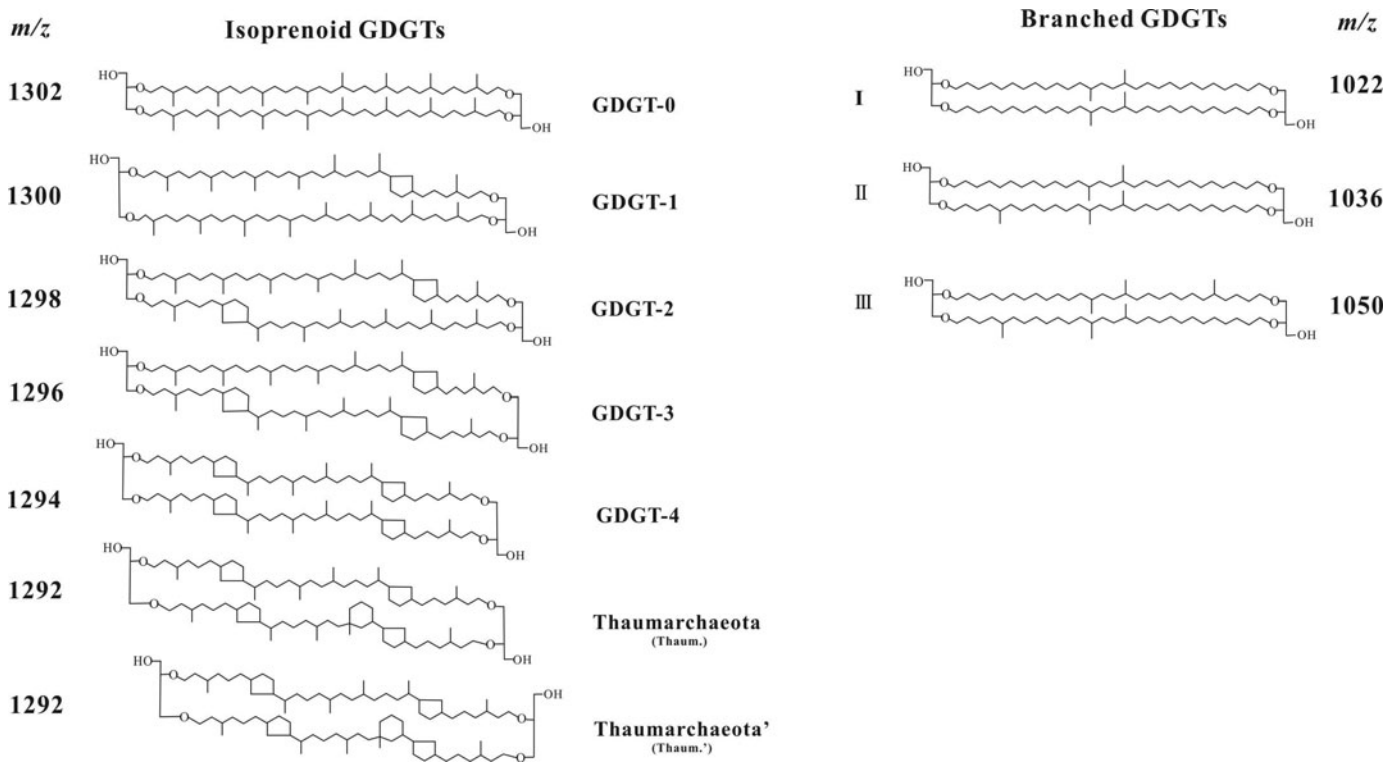

Fig. 1. Structures of archaeal lipids in this study. GDGT: glycerol dibiphytanyl glocerol tetraethers.

2008) and changes in nutrients and pH (Pearson et al. 2008; Turich et al. 2007b), which may compromise the application of TEX_{86} as an SST proxy (Turich et al. 2007). TEX_{86} also can be biased by GDGT inputs from soil archaea (Weijers et al. 2006; Zhu et al. 2011) and benthic archaea in hydrate rich environments (Liu et al. 2011; Zhang et al. 2011). Furthermore, other studies have shown that TEX_{86} values for intact polar lipid (IPL) GDGTs are consistently higher than those from core lipid GDGTs even in normal marine sediments (Lipp and Hinrichs 2009; Wei et al. 2011).

Mass-transported deposits (MTDs) are an important component of deep water deposition system, which often occur in deep water basins around the world and play an important role in petroleum exploration and production (Moscardelli and Wood, 2008; Shao et al. 2010; Wang et al., 2009). The South China Sea (SCS) is the largest marginal sea of the western Pacific Ocean. The Qiongdongnan Basin is located in the present shelf, slope and abyssal environments (Xie et al. 2006) with the slope environment containing one of the gas hydrate prospecting zones in the northern SCS (Yang et al. 2013). Wang et al. (2009) showed that MTDs are widely distributed in Quaternary sedimentary sequences of the continental slope in the Qiongdongnan Basin of SCS. Many paleoclimate studies have been conducted in the SCS, which are commonly based on temperature proxies such as foraminiferal oxygen isotope ratios and Mg/Ca ratios, foraminiferal transfer function, or the U^{K}_{37} methods (Jian et al. 2000; Jian et al. 2003; Zhao et al. 2006). Recently, the TEX_{86} proxy has been used to reconstruct temperature records in SCS (Ge et al. 2013; Jia et al. 2012; Li et al. 2013; Wei et al. 2011; Zhang et al. 2013), however, the impact of MTDs on plaeoclimate records, especially on the TEX_{86} index, is poorly known.

In this study, we analyzed GDGT lipids and molecular DNA from sediments in the Qiongdongnan Basin of the SCS. We also compared polar (P)-GDGT contents that were measured by liquid chromatography-mass spectrometry (LC-MS) to those calculated from archaeal 16S rRNA gene copies (a proxy for cell abundance) in order to evaluate the effect of intact polar GDGTs in sediments on TEX_{86}. Our results show that despite the samples being from the hydrate-rich region, the lipids in the sediments are predominantly from planktonic archaea, and the calculated TEX_{86} indicates winter sea surface temperature during the last 24 Ka years. The effect of MTDs on TEX_{86} is also evaluated in this study.

Material and Methods

Site Description and Sampling

A sediment core (HQ08-48PC; 16°57.5134′N, 110°31.5809′ E, 1,474 m; Figure 2) was obtained during the cruise HY4-2008-1 in the Qiongdongnan Basin of the northern SCS. Sediment samples were collected using the R/V Haiyang No. 4. The core was 7.14 m long, soft, rich in foraminifera and made up of silty clay. Eleven sediment samples were obtained aseptically with each sample collected every 70 cm along the core. These samples were collected into 50-mL centrifuge tubes and stored at −80°C until analysis.

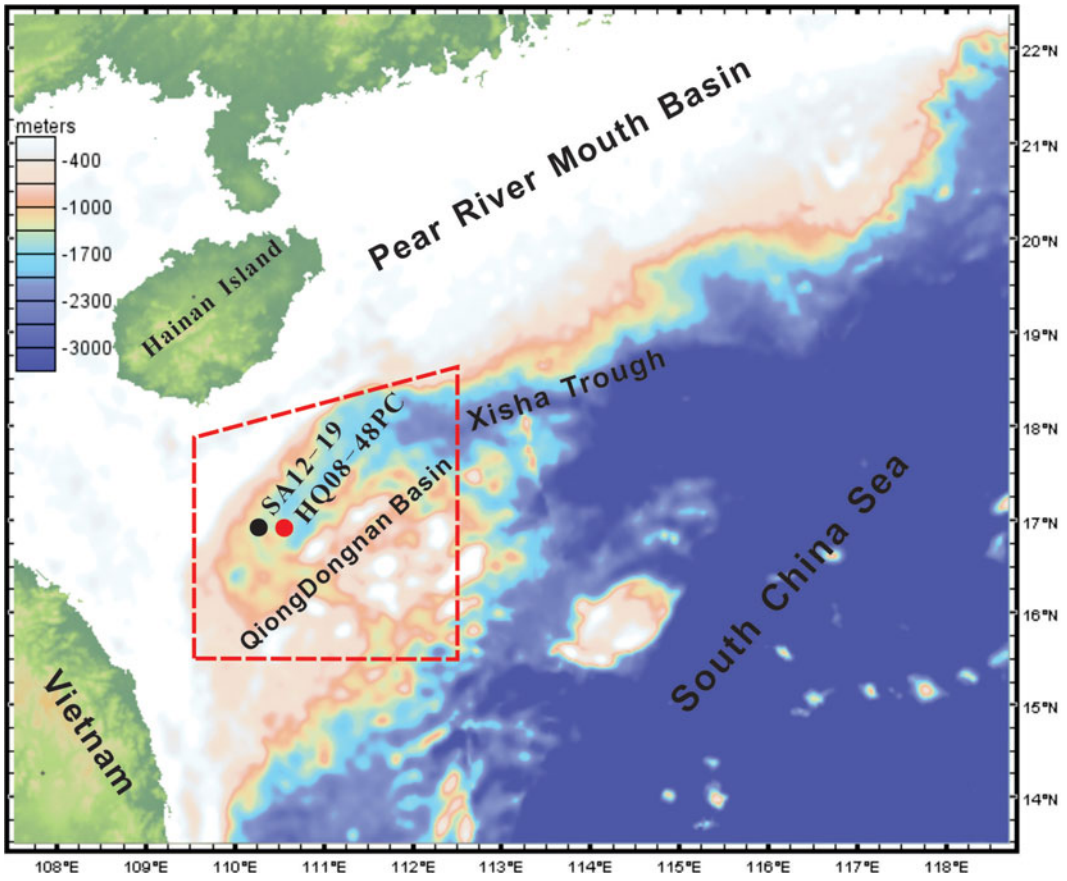

Fig. 2. Map showing the location of core HQ08-48PC in this study. Blue dot is from a previous study (Jiang and Li 2003).

Environmental and Bulk Parameter Analysis

Pore water

Pore waters were obtained by centrifuging the sediments and were filtered through a 0.22-μm pore size, 4-mm diameter filter prior to analysis. Sulfate and chlorine were analyzed with an Ion Chromatogram (DX-600, Dionex, USA). Methane was analyzed using a Gas Chromatograph (6890 N series, Agilent Technologies, USA) on board the ship.

TOC, TN and carbon isotopes of TOC

About 5-g sediment was decarbonated using 10% HCl and neutralized by repeated washing with distilled and deionised water before analysis. Part of the dried bulk sediment was used for analysis of total organic carbon (TOC) using an element analyzer (EA1110, Carlo Erba). The carbon isotopes of the TOC were then determined on the GV-Isoprime EA IRMS with a precision of 0.1‰ for δ^{13}C (VPDB), which is defined as

$$\delta^{13}\mathrm{C} = [(^{13}\mathrm{C}/^{12}\mathrm{C})\mathrm{sa}/(^{13}\mathrm{C}/^{12}\mathrm{C})\mathrm{std} - 1] \times 1000$$

where "sa" stands for sample and "std" for standard.

DNA Analysis

DNA isolation and amplification

Bulk DNA was extracted from sediment samples using PowerSoil DNA Isolation Kit (Mo Bio Laboratories, Carlsbad, CA) in accordance with the manufacturer's instructions. Archaeal 16S rRNA gene fragments were amplified using primers Arch21F (5′-TTCCGGTTG ATCCYGCCGCCGGA-3′) and Arch958R (5′-YCCGGC GTTGAMTCCAATT-3′) as previous described (DeLong 1992). The conditions for amplification of archaeal 16S rRNA genes were the following: initial denaturation at 95°C for 3 min; 30 cycles of denaturing (1 min at 94°C), annealing (1 min at 55°C), and extension (1.5 min at 72°C); and a final extension at 72°C for 10 min. The PCR products were purified with a QIAquick PCR Purification kit (Qbiogene Inc., Irvine, CA) according to the manufacturer's suggested protocol.

Quantitative PCR

Quantitative PCR was performed using the StepOne real-time system (Life Technologies) and a 20 μl reaction mixture that consisted of 2 μl (1 to 10 ng) of DNA as the template, 0.4 μl (10 μM) of each primer, 0.4 μl ROX Reference Dye (50×) and 10 μl of SYBR® *Premix Ex Taq* (2×) (TAKARA). Archaeal 16S rRNA genes were quantified using the primers 344F (5′-ACGGGGCGCAGCAGGCGCGA-3′) and 518R

(5′-ATTACCGCGGCTGCTGG-3′) (Ovreas et al. 1998) and the following thermal profile: 30 sec at 95°C, followed by 40 cycles of 5 sec at 95°C, 1 min at 60°C; 15 sec at 95°C, 1 min at 60°C, and 15 sec at 95°C to make the melting curve.

Cloning and restriction fragment length polymorphism (RFLP) analysis

The PCR product was ligated into the pMD-18T vector (TaKaRa) and transformed into *Escherichia coli* DH5α competent cells. The transformed cells were plated on Luria-Bertani plates containing 100 μg/mL of ampicillin, 80 μg/mL of X-Gal (5-bromo-4-chloro-3-indolyl-β-D-galactopyranoside), and 0.5 mM IPTG (isopropyl-β-D-thiogalactopyranoside) and incubated overnight at 37°C. Resulting PCR products were screened for the correct size and purity by 1% agarose gel electrophoresis.

The PCR-amplified inserts were digested with the restriction endonucleases MspI (Fermentas) for 3 h at 37°C. The resulting products were separated by gel electrophoresis on a 3.0% agarose gel in TAE buffer. A total of 206 clones were analyzed and at least one phylotype from each group (determined by RFLP banding pattern and/or $\geq$ 97 sequence similarity) was subject to complete nucleotide sequencing.

Phylogenetic analysis

The 16S rRNA gene sequences were grouped into operational taxonomic units (OTUs) at 3% distance cut-off using the DOTUR program (Schloss and Handelsman 2005). Sequence similarity searches were performed using the BLAST network service of the NCBI database (http://www.ncbi.nlm.nih.gov/BLAST). The sequences were tested for chimeras by using the Ribosomal Database Project Chimera-Check program and were aligned with Clustal W (Thompson et al. 1997). Phylogenetic trees were constructed using the MEGA program version 3.0 (Kumar et al. 2004) with the Kimura two-parameter algorithm and the neighbor-joining method.

Accession number of nucleotide sequences

The sequences have been deposited in the GenBank database under accession numbers: HQ611174 - HQ611227.

Lipid Extraction and Analysis

The original sample was spiked with an internal standard (C_{46}, 974.08 ng) before the extraction procedure began. The freeze-dried sediment sample spiked with the internal standard was extracted ultrasonically five times with a mixture of dichloromethane (DCM): methanol (MeOH) (3:1, v/v). The total extract was transferred into a KOH-MeOH solution (6%) for overnight and then extracted by *n*-hexane five times. Lipid analysis by HPLC-MS followed previously described procedures (Wei et al. 2011).

Briefly, the GDGTs were first eluted isocratically with (A) *n*-hexane and (B) isopropanol as follows, 99% A: 1% B for 5 min, then a linear gradient to 1.8% B in 45 min. Flow rate was 0.2 mL/min. After each analysis the column was cleaned by back flushing with *n*-hexane/isopropanol (90:10, vol: vol) at 0.2 mL/min for 10 min. Conditions for APCI/MS were as follows: nebulizer pressure 60 psi, vaporizer temperature 400°C, drying gas (N_2) flow 5 L/ min and temperature 200°C, capillary voltage −3.5 kV, corona 5 μA (3.2 kV). Single ion monitoring (SIM) mode was used to detect eight isoprenoidal GDGT signals (m/z 1302, 1300, 1298, 1296, 1292, 1050, 1036, 1022) and the C_{46} internal standard (m/z 744), with a dwell time of 237 ms per ion.

GDGT Proxies

(1) TEX_{86} was calculated based on the equation from Schouten et al. (2002) and Kim et al. (2010):

$$TEX_{86} = \frac{\text{GDGT-2} + \text{GDGT-3} + \text{Thaum.}'}{\text{GDGT-1} + \text{GDGT-2} + \text{GDGT-3} + \text{Thaum.}'}$$

$$TEX_{86}^{H} = \log\frac{\text{GDGT-2} + \text{GDGT-3} + \text{Thaum.}'}{\text{GDGT-1} + \text{GDGT-2} + \text{GDGT-3} + \text{Thaum.}'}$$

(2) TEX_{86}-derived sea surface temperatures (SST) were calculated according to Kim et al. (2010):

$$SST = 68.4 \times TEX_{86}^{H} + 38.6$$

(3) BIT and MI index were calculated according to Hopmans et al. (2004) and Zhang et al. (2011), respectively:

$$BIT = \frac{\text{I} + \text{II} + \text{III}}{\text{I} + \text{II} + \text{III} + \text{Thaum.}}$$

$$MI = \frac{\text{GDGT-1} + \text{GDGT-2} + \text{GDGT-3}}{\text{GDGT-1} + \text{GDGT-2} + \text{GDGT-3} + \text{Thaum.} + \text{Thaum.}'}$$

GDGT Abundance Calculated from Cell Numbers

We assumed that each living archaeal cell would contain one 16S rRNA gene and the GDGT per cell maximum would be 8.5 fg IP-GDGT cell^{-1} (Huguet et al. 2010). Thus IP-GDGT abundances were calculated on the basis of the archaeal 16S rRNA gene copy numbers.

Results and Discussion

Geochemical and Biological Profiles Supporting the Applicability of TEX_{86} in the SCS

Because the Qiongdongnan Basin is one of the most prospective areas for gas hydrate explorations in the northern continental slope of the SCS, TEX_{86}-derived temperatures may not be valid where high rates of anaerobic oxidation of methane occur (Pancost et al. 2001; Schouten et al. 2002; Wakeham et al. 2007; Zhang et al. 2011). Thus geochemistry profiles were first obtained to evaluate the application of TEX_{86} in this region of the northern SCS.

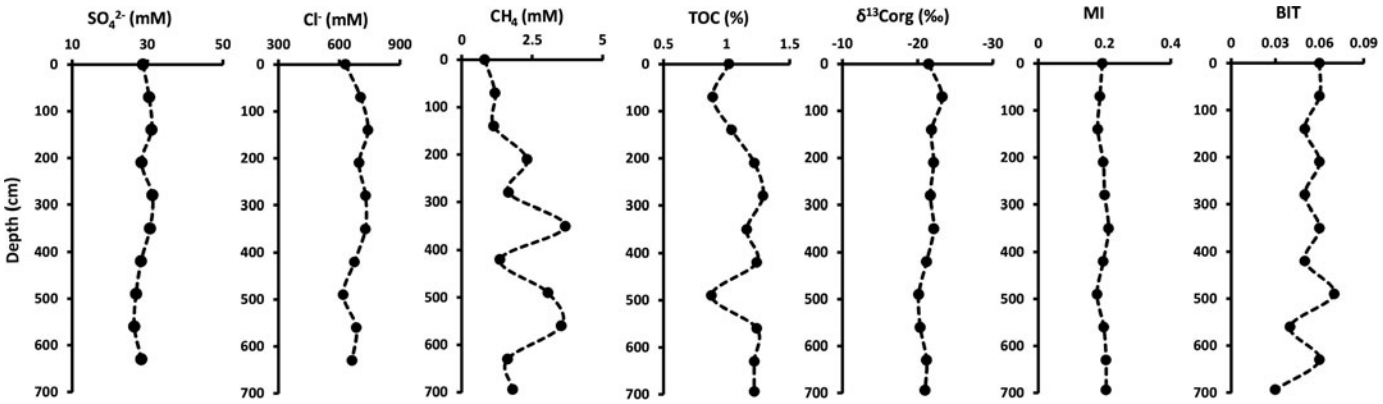

Fig. 3. Depth profiles of sulfate, chloride, methane, TOC, stable carbon isotopes and calculated MI.

The CH_4 concentrations in all samples ranged from 0.82 to 3.68 mM (Figure 3, Supplementary Table S1), which are in the lower end of normal marine sediments (Van Dover 2000) and were low compared to methane concentrations in hydrate locations (Levin 2005).

Porewater sulfate concentrations ranged from 26.49 to 31.31 mM, indicating low activity of sulfate reduction; the Cl^- concentrations ranged from 620.3 to 742.6 mM, indicating a lack of hydrate dissociation that may release fresh water to dilute the Cl^- concentration (Figure 3, Supplementary Table S1). The TOC concentrations ranged from 0.88 to 1.29% and the $\delta^{13}C$ of TOC remained relatively constant averaging −21.49‰ (Figure 3, Supplementary Table S1), which indicates a signature of normal marine TOC. This is further supported by the MI values (0.18 to 0.21), which are in the range of 0–0.3 for normal marine conditions (Zhang et al. 2011). BIT values were less than 0.2 in all samples (Figure 3), which are in the range of open marine sediments (Hopmans et al. 2004).

We also investigated the archaeal diversity and community structures that provided independent information on methane oxidation by archaea. All the archaeal sequences belonged to either Crenarchaeota/Thaumarcheoata or Euryarchaeaota (Figure 4a, Supplementary Table S2). The former group consisted of Marine Group I (MGI) of Thaumarchaeota, and Miscellaneous Crenarchaeotal Group (MCG), Marine Benthic Group A (MBGA), Marine Benthic Group B (MBGB) and C3 of Crenarcheota (Figure 4a, Supplementary Table S2). The other group consisted of the Marine Benthic Group D (MBGD), the South African Gold Mine Euryarchaeotal Group (SAGMEG), Novel Euryarchaeotic Group (NEG), Miscellaneous Euryarchaeotal Group (MEG), Deep-Sea Hydrothermal Vent Euryarchaeotic Group 6 (DHVE6) and the Marine Benthic Group E (MBGE) of Euryarchaeota (Figure 4a, Supplementary Table S2).

Archaeal community structure changed with depth along the sediment core (Figure 4a). The upper layer was dominated by uncultivated archaeal lineages (38% of MGI and 26% of MBGB), the intermediate layer had the archaeal lineages relatively evenly distributed (35% of MBGB, 20% of MCG, 20% of MBGD and 16% of C3), and the deeper layer was mainly composed of uncultivated archaeal lineages (51% of MCG and 34% of MBGD) (Figure 4a, Supplementary Table S2).

MCG and MBGD increased in phylotypes with increasing depth of the core, indicating their potential importance in deeper marine subsurface. However, none of the samples showed the presence of ANME groups that are associated with anaerobic oxidation of methane commonly occurring in cold seep or gas hydrate locations (Harrison et al. 2009; Knittel et al. 2005; Teske et al. 2002).

Collectively, the low CH_4 concentrations, relatively high concentrations of porewater sulfate, $\delta^{13}C$ of TOC characteristic of nonmethane oxidation and low MI, and the lack of ANME groups suggest that sediment in core HQ08-48PC was deposited under normal marine conditions. Therefore, the TEX_{86}-derived temperatures from our samples were unlikely to be biased by methane-metabolizing archaea (Zhang et al. 2011).

IP-GDGT Effect on TEX_{86} of C-GDGT

GDGT distribution

All samples showed a characteristic marine archaeal GDGT profile, with abundant thaumarchaeol (51.5–60.8%) and GDGT-0 (20.0–30.3%) and less contributions of GDGT-1 to GDGT-3 and the thaumarchaol regioisomer among the different samples. This observation was consistent with our previous findings in the SCS (Ge et al. 2013; Wei et al. 2011). Cluster analysis showed that the compositions of the archaeal C-GDGTs in the post glacial (PG) period were clearly different from those in the Last Glacial Maximum (LGM) period (Figure 5).

IP-GDGT Effect on TEX_{86} of C-GDGT

The number of archaeal 16S rRNA genes in our samples averaged 22.1×10^4 copies/g (n = 11) and ranged from 108.0×10^4 to 4.1×10^4 copies/g (wet weight) (Figure 6). The archaeal copies reached the highest value of 108.0×10^4 copies/g (wet weight) in the uppermost sample.

IP-GDGT abundance calculated according to archaeal 16S rRNA gene copies ranged from 0.4 to 9.2 ng/g (Figure 6).

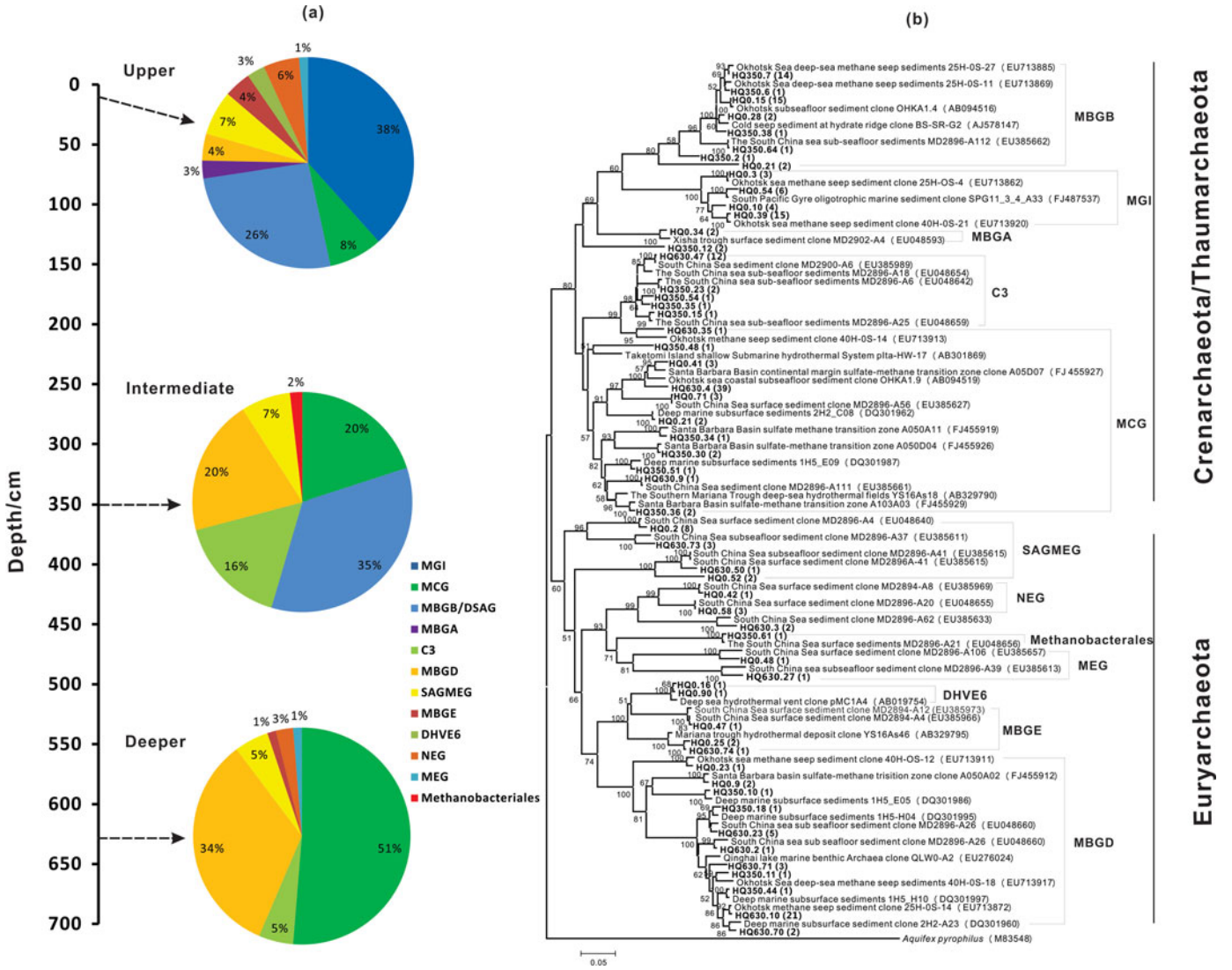

Fig. 4. Frequency of the archaeal lineages and Neighbor-joining tree of the archaeal 16S rRNA genes. (a) Frequency of archaeal lineages in clone libraries constructed from samples collected at 0–20 cm, 350–370 cm and 630–650 cm in the sediment core HQ08-48PC. (b) Phylogenetic tree constructed using archaeal 16S rRNA genes recovered from the upper, intermediate and deeper sediments of the core. The unique archaeal 16S rRNA sequences obtained in this study were grouped at 0.03 distance cutoff using the DOTUR program. The scale bar represents a 5% sequence difference. The archaeal 16S rRNA sequences obtained in this study are shown in bold, along with their distribution in each clone library as depicted in the parentheses.

In contrast, C-GDGT abundance averaged 705.6 ng/g (n = 11) and ranged from 378.7 to 1055.7 ng/g (Figure 6). The calculated IP-GDGT abundance was thus several orders of magnitude lower than that of C-GDGT. This is consistent with results from Lengger et al. (2012) who compared IP-GDGT with C-GDGT by direct LC-MS analysis.

TEX_{86} value can be affected by IPL derived from in situ production by benthic heterotrophic archaea in sediments (Lipp and Hinrichs 2009). Some studies showed that TEX_{86} values for IPL GDGTs were consistently higher than those from core lipid GDGTs (Lipp and Hinrichs 2009; Liu et al. 2011; Wei et al. 2011). In this study, abundance of IP is less than 1% of total GDGTs, which suggests that in situ production in the subsurface sediment does not substantially influence the TEX_{86} of the C-GDGT.

Indication of TEX_{86} SST

The SST derived from TEX_{86} was calculated according to Kim et al. (2010) and ranged from 21.1°C to 27.4°C along the sediment core. TEX_{86} SST had a narrow range of 26.7 to 27.4°C between 0 and 140 cm, following a rapid decrease to 21.2°C from 140 cm to 280 cm and then maintained a relatively constant value of 21.3°C (Figure 7). A sediment core (SA12-19) near HQ08-48PC had been drilled for paleoclimate study, and foraminiferal transfer functions (Jiang and Li 2003)

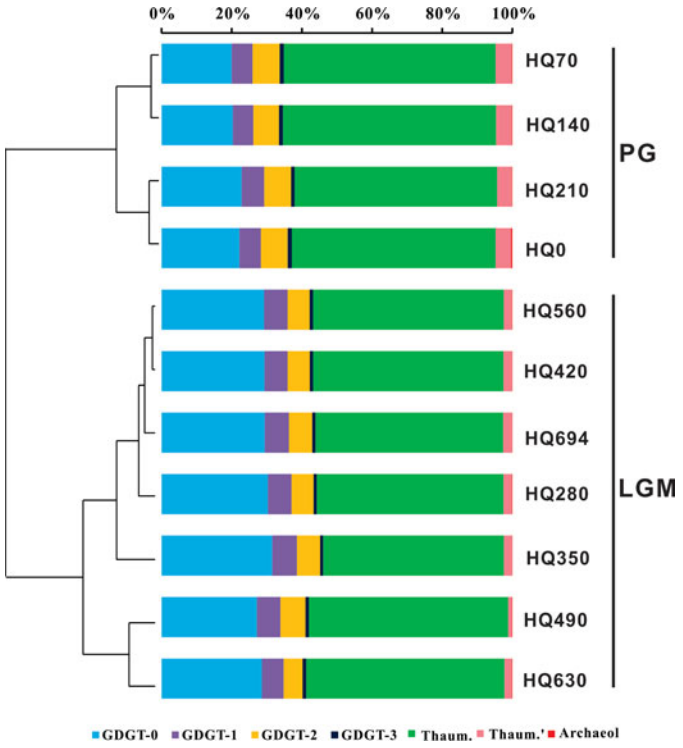

Fig. 5. Clustering analysis of relative abundances of GDGTs in archaeal core lipids from HQ08-48PC of the South China Sea. PG and LGM stand for Post Glacial and the last Glacial Maximum period, respectively.

showed distinct winter and summer SSTs changes during the last glacial-Holocene transition (Figure 7). Supposing that HQ08-48PC and SA12-19 had the same sedimentary rate because both cores were very close and had similar water depth, the age model of core SA12-19 was applied to core HQ08-48PC.

The SST derived from TEX_{86} in this study agrees in general with the winter temperature recorded by planktonic foraminiferas (Jiang and Li 2003); however, a large difference can occur at different depths (Figure 7). There may be several possibilities for the difference between the two temperature proxies.

First, samples of TEX_{86} proxy has lower resolution than those of planktonic foraminifera (PF)-based temperatures so that some detail temperature changes were not revealed in core HQ08-48PC. The sampling interval for TEX_{86} was 70 cm; whereas the sampling interval for PF-based temperature was 10 cm in average. Second, the standard deviation of TEX_{86} temperature was 2.5°C whereas the standard deviation of PF-based temperature was 1.39°C (Jiang and Li 2003). However, the largest difference between TEX_{86} and PF-based winter temperature is >4°C, which cannot be explained by the poor resolution of the TEX_{86}. Third, TEX_{86} may be a mixed signal of archaeal biomass from different water depths or seasons. Previous studies have indicated that TEX_{86} values may reflect a specific season of the year in different sites (Schouten et al. 2013).

Leider et al. (2010) showed that the TEX_{86}-based temperatures reflected winter SSTs for the nearshore sites on the southern Italian shelf but corresponded to summer SSTs at

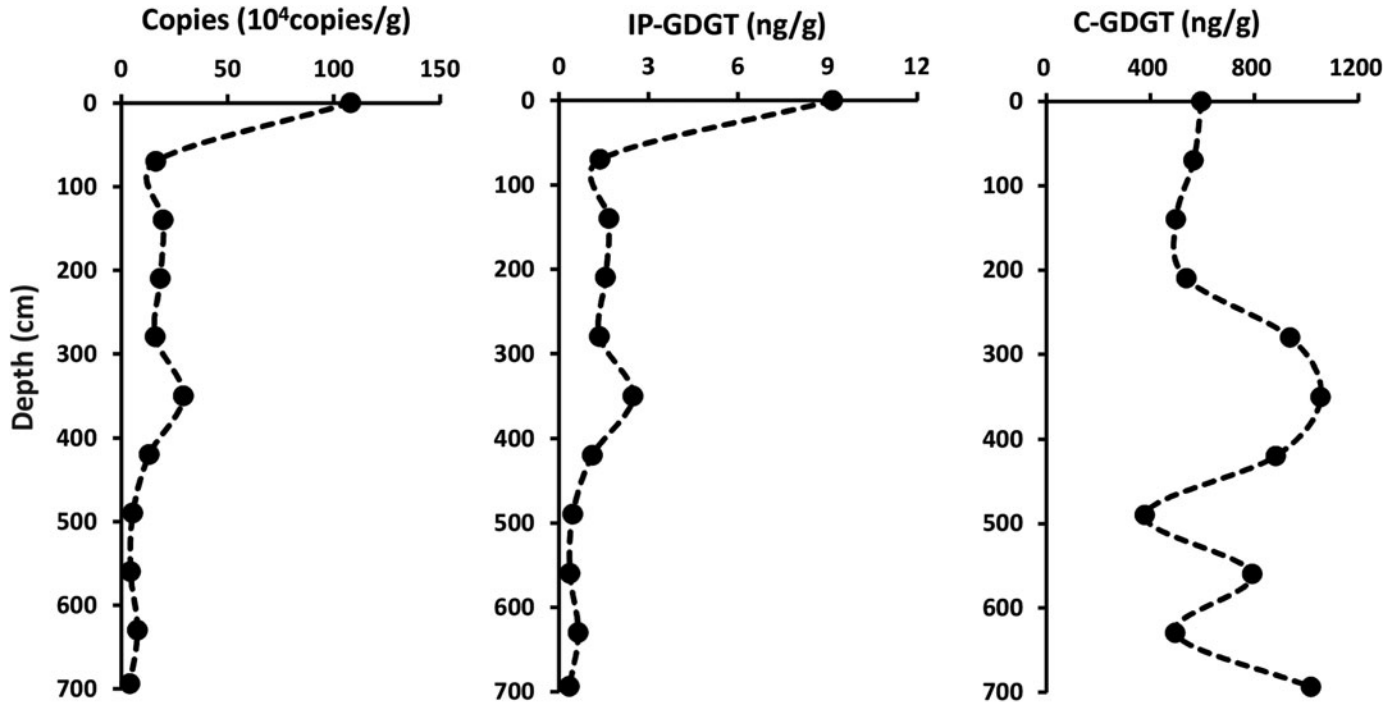

Fig. 6. Depth profiles of archaeal 16S rRNA gene copies and GDGT lipid contents. 16S rRNA gene copies were obtained using quantitative PCR; IP-GDGT was calculated on the basis of the archaeal 16S rRNA gene copy numbers and single cell GDGT lipid content (Huguet et al. 2010); The content of C-GDGTs were analyzed using LC-MS directly.

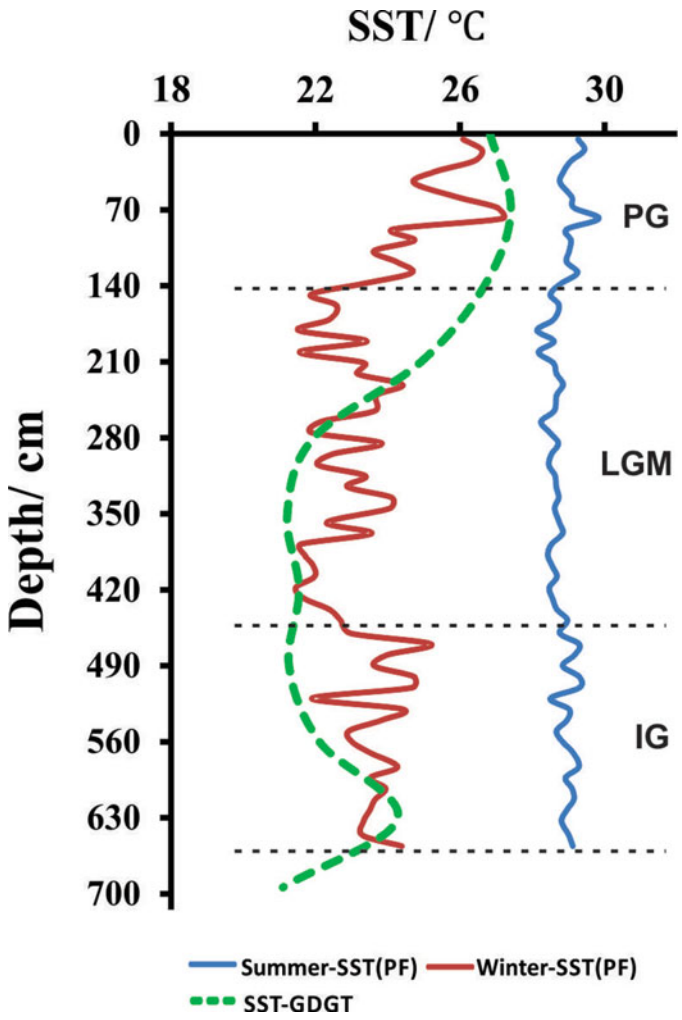

Fig. 7. Paleo temperature variation since the last glacial maxima in the northern SCS. TEX_{86}-based SST was reconstructed according to Kim et al. (2010) from the Core HQ08-48PC (in green dash line); SSTs in winter (red line) and summer (blue line) were calculated based on planktonic foraminifera (PF) in core SA12-19 using palaeoecological transfer functions (Jiang and Li 2003).

the most offshore sites (>733 m). Ge et al. (2013) and Zhang et al. (2013) also showed that TEX_{86}-based temperature values near shore reflect winter SST in the northern SCS. It also has been argued that the sediment GDGTs are deposited from the whole water column above the sediment (Schouten et al. 2002; Wuchter et al. 2006). In the SCS, previous studies have also suggested that the TEX_{86} index reflect subsurface temperature (Jia et al. 2012; Li et al. 2013), which would be lower than summer SST, but possibly close to winter SST for the site. Fourth, the core may be a mixture of shallow and deep water sediments as a result of MTDs.

Wang et al. (2009) show that MTDs are widely distributed in Quaternary sedimentary sequences of the continental slope in the Qiongdongnan Basin of SCS and led to effective transport of shallow sediment to the deep water (Li et al. 2011; Wang et al. 2009), suggesting the GDGTs signals may have originated mainly from near shore sediments. The core indeed recorded mostly near shore environment in the northern continental slope of the SCS, which is also supported by the high input of land-derived material from the near shore in the northern SCS (Chen et al. 1998; Shao et al. 2010; Xie et al. 2006). Overall, the discrepancy between TEX_{86} proxy and the PF proxy indicate the complex hydrological and depositional environment in the Qiongdongnan Basin.

It is important to notice that MTDs affect TEX_{86} in continental margins. Further work is necessary to better understand sediment depositional and transport processes from near shore to open oceans in the marginal sea and thus to better understand the changes in past sea temperature during geological history.

Conclusions

In this study we employed molecular DNA and lipid biomarker approaches to evaluate IP-GDGT effect on TEX_{86} in a hydrate-prospect zone in the South China Sea. The results showed that the sediment core had little impact of hydrate dissociation and the archaeal community structures exhibited significant change with depth with IP-GDGTs being too small a quantity to affect TEX_{86} values derived from C-GDGTs. Therefore, the fossil archaeal lipids reasonably recorded the changes in past sea temperature of the near shore environment in the SCS since the last glacial maxima, which agrees generally with the winter temperature recorded by planktonic foraminiferas collected from the same area of the SCS. However, due to the complex hydrological and depositional conditions of the Qiongdongnan basin, the TEX_{86} proxy should be used with caution in this geological unstable region.

Acknowledgments

The sediment samples used in this study were collected during the 2007 South China Sea Open Cruise by R/V Shiyan 3, South China Sea Institute of Oceanology, CAS. All procedures on samples were performed at the State Key Laboratory of Marine Geology at Tongji University. We thank Lei Shao for advice on the sedimentology of the Qiongdongnan Basin in the northern South China Sea and the two anonymous reviewers for constructive comments that improved the quality of an early version of the article.

Funding

This research was supported by the National Science Foundation of China Grant No. 40730844 (MZ) and by the South China Sea-Deep program of the National Science Foundation of China Grant No. 91028005 (CLZ) and the "National Thousand Talents Program" at the State Key Laboratory of Marine Geology of Tongji University.

Supplemental Material

Supplemental data for this article can be accessed on the publisher's website.

References

Boyd ES, Pearson A, Pi Y, Li WJ, Zhang YG, He L, et al. 2011. Temperature and pH controls on glycerol dibiphytanyl glycerol tetraether lipid composition in the hyperthermophilic crenarchaeon *Acidilobus sulfurireducens*. Extremophiles 15:59–65.

Castañeda IS, Schefuss E, Sinninghe Damsté JS, Weldeab S, Schouten S. 2010. Millennial-scale sea surface temperature changes in the eastern Mediterranean (Nile River Delta region) over the last 27,000 years. Paleoceanography 25:PA1208.

Chen H, Li S, Sun Y, Zhang Q. 1998. Two petroleum systems charge the YA13-1 gas field in Yinggehai and Qiongdongnan basins, South China Sea. AAPG Bull-Amer Asso Petrol Geol 82:757–772 (In Chinese).

DeLong EF. 1992. Archaea in coastal marine environments. Proc Natl Acad Sci USA 89:5685–5689.

Ge HM, Zhang CL, Dang HY, Zhu C, Jia GD. 2013. Distribution of tetraether lipids in surface sediments of the northern South China Sea: Implications for TEX_{86} proxies. Geosci Front 4:223–229.

Harrison BK, Zhang H, Berelson W, Orphan VJ. 2009. Variations in archaeal and bacterial diversity associated with the sulfate-methane transition zone in continental margin sediments (Santa Barbara Basin, California). Appl Environ Microbiol 75:1487–1499.

Herfort L, Schouten S, Boon JP, Sinninghe Damsté JS. 2006. Application of the TEX_{86} temperature proxy to the southern North Sea. Organ Geochemi 37:1715–1726.

Hopmans EC, Weijers JWH, Schefuß E, Herfort L, Sinninghe Damsté JS, Schouten S. 2004. A novel proxy for terrestrial organic matter in sediments based on branched and isoprenoid tetraether lipids. Earth Planet Sci Lett 224:107–116.

Huguet C, Martrat B, Grimalt JO, Sinninghe Damsté JS, Schouten S. 2011. Coherent millennial-scale patterns in $U^{K'}_{37}$ and TEX^{H}_{86} temperature records during the penultimate interglacial-to-glacial cycle in the western Mediterranean. Paleoceanography 26: PA2218.

Huguet C, Urakawa H, Martens-Habbena W, Truxal L, Stahl DA, Ingalls AE. 2010. Changes in intact membrane lipid content of archaeal cells as an indication of metabolic status. Organ Geochem 41:930–934.

Jia GD, Zhang J, Chen JF, Peng PA, Zhang CL. 2012. Archaeal tetraether lipids record subsurface water temperature in the South China Sea. Organ Geochem 50:68–77.

Jian ZM, Li BH, Huang BQ, Wang JL. 2000. Globorotalia truncatulinoides as indicator of upper-ocean thermal structure during the Quaternary: evidence from the South China Sea and Okinawa Trough. Palaeogeogr Palaeoclimatol Palaeoecol 162:287–298.

Jian ZM, Zhao QH, Cheng XR, Wang JL, Wang PX, Su X. 2003. Pliocene-Pleistocene stable isotope and paleoceanographic changes in the northern South China Sea. Palaeogeogr Palaeoclimatol Palaeoecol 193:425–442.

Jiang MS, Li XJ. 2003. Planktonic foraminifera and sea surface temperature (SST) of the Xisha Trough, South China Sea since last glaciation. Sci China Ser D-Earth Sci 46:1–9.

Kim JH, Crosta X, Michel E, Schouten S, Duprat J, Sinninghe Damsté JS. 2009. Impact of lateral transport on organic proxies in the Southern Ocean. Quatern Res 71:246–250.

Kim JH, Schouten S, Hopmans EC, Donner B, Sinninghe Damsté JS. 2008. Global sediment core-top calibration of the TEX_{86} paleothermometer in the ocean. Geochim Cosmochim Acta 72:1154–1173.

Kim JH, van der Meer J, Schouten S, Helmke P, Willmott V, Sangiorgi F, Koç N, Hopmans EC, Sinninghe Damsté JS. 2010. New indices and calibrations derived from the distribution of crenarchaeal isoprenoid tetraether lipids: Implications for past sea surface temperature reconstructions. Geochim Cosmochim Acta 74:4639–4654.

Knittel K, Losekann T, Boetius A, Kort R, Amann R. 2005. Diversity and distribution of methanotrophic archaea at cold seeps. Appl Environ Microbiol 71:467–479.

Kumar S, Tamura K, Nei M. 2004. MEGA3: Integrated software for Molecular Evolutionary Genetics Analysis and sequence alignment. Brief Bioinform 5:150–163.

Lai D, Springstead JR, Monbouquette HG. 2008. Effect of growth temperature on ether lipid biochemistry in Archaeoglobus fulgidus. Extremophiles 12:271–278.

Leider A, Hinrichs KU, Mollenhauer G, Versteegh GJM. 2010. Core-top calibration of the lipid-based $U^{K'}_{37}$ and TEX_{86} temperature proxies on the southern Italian shelf (SW Adriatic Sea, Gulf of Taranto). Earth Planet Sci Lettt 300:112–124.

Lengger SK, Hopmans EC, Reichart G-J, Nierop KG, Sinninghe Damsté JS, Schouten S. (2012) Intact polar and core glycerol dibiphytanyl glycerol tetraether lipids in the Arabian Sea oxygen minimum zone. Part II: Selective preservation and degradation in sediments and consequences for the TEX86. Geochimica et Cosmochimica Acta 98:244–258.

Levin LA. 2005. Ecology of cold seep sediments: interactions of fauna with flow, chemistry and microbes. Oceanogr Mar Biol Ann Rev 43:1–46.

Li D, Wang YM, Wang YF, Xu Q. 2011. Identification of mass transport complexes and their implications for hydrocarbon exploration: An example from the Central Canyon area in southeastern Hainan Basin. Sediment Geol Tethyan Geol 3:58–63 (In Chinese).

Li DW, Zhao MX, Tian J, Li L. 2013. Comparison and implication of TEX_{86} and $U^{K'}_{37}$ temperature records over the last 356kyr of ODP Site 1147 from the northern South China Sea. Palaeogeog Palaeoclimatol Palaeoecol 376:213–223.

Lipp JS, Hinrichs KU. 2009. Structural diversity and fate of intact polar lipids in marine sediments. Geochim Cosmochim Acta 73:6816–6833.

Liu XL, Lipp JS, Hinrichs KU. 2011. Distribution of intact and core GDGTs in marine sediments. Organ Geochem 42:368–375.

Moscardelli L, Wood L. 2008. New classification system for mass transport complexes in offshore Trinidad. Basin Res 20:73–98.

Ovreas L, Jensen S, Daae FL, Torsvik V. 1998. Microbial community changes in a perturbed agricultural soil investigated by molecular and physiological approaches. Appl Environ Microbiol 64: 2739–2742.

Pancost RD, Bouloubassi I, Aloisi G, Sinninghe Damsté JS, Scientific Party TMS 2001. Three series of non-isoprenoidal dialkyl glycerol diethers in cold-seep carbonate crusts. Organ Geochem 32:695–707.

Pearson A, Pi Y, Zhao W, Li W, Li Y, Inskeep W, Perevalova A, Romanek C, Li S, Zhang CL. 2008. Factors controlling the distribution of archaeal tetraethers in terrestrial hot springs. Appl Environ Microbiol 74:3523–3532.

Schleper C, Jurgens G, Jonuscheit M. 2005. Genomic studies of uncultivated archaea. Nat Rev Microbiol 3:479–488.

Schloss PD, Handelsman J. 2005. Introducing DOTUR, a computer program for defining operational taxonomic units and estimating species richness. Appl Environ Microbiol 71:1501–1506.

Schouten S, Hopmans EC, Sinninghe Damsté JS. 2013. The organic geochemistry of glycerol dialkyl glycerol tetraether lipids: A review. Organ Geochem 54:19–61.

Schouten S, Hopmans EC, Pancost RD, Sinninghe Damsté JS. 2000. Widespread occurrence of structurally diverse tetraether membrane lipids: evidence for the ubiquitous presence of low-temperature relatives of hyperthermophiles. Proc Natl Acad Sci USA 97:14421–14426.

Schouten S, Hopmans EC, Schefuss E, Sinninghe Damsté JS. 2002. Distributional variations in marine crenarchaeotal membrane lipids: a new tool for reconstructing ancient sea water temperatures? Earth Planet Sci Lett 204:265–274.

Schouten S, Huguet C, Hopmans EC, Sinninghe Damsté JS. 2007. Improved analytical methodology of the TEX_{86} paleothermometry by high performance liquid chromatography atmospheric pressure chemical ionization-mass spectrometry. Anal Chem 79:2940–2944.

Shah SR, Mollenhauer G, Ohkouchi N, Eglinton TI, Pearson A. 2008. Origins of archaeal tetraether lipids in sediments: Insights from radiocarbon analysis. Geochim Cosmochim Acta 72:4577–4594.

Shao L, Li A, Wu G, Li Q, Liu C, Qiao P. 2010. Evolution of sedimentary environment and provenance in Qiongdongnan Basin in the northern South China Sea. Acta Petrolei Sinica 31:548–552 (In Chinese).

Sinninghe Damsté JS, Rijpstra WIC, Reichart G-J. 2002. The influence of oxic degradation on the sedimentary biomarker record II. Evidence from Arabian Sea sediments. Geochim Cosmochim Acta 66:2737–2754.

Teske A, Hinrichs KU, Edgcomb V, de Vera Gomez A, Kysela D, Sylva SP, et al. 2002. Microbial diversity of hydrothermal sediments in the Guaymas Basin: evidence for anaerobic methanotrophic communities. Appl Environ Microbiol 68:1994–2007.

Thompson JD, Gibson TJ, Plewniak F, Jeanmougin F, and Higgins, DG 1997. The CLUSTAL_X windows interface: flexible strategies for multiple sequence alignment aided by quality analysis tools. Nucleic Acids Res 25:4876–4882.

Turich C, Freeman KH, Bruns MA, Conte M, Jones AD, Wakeham SG. 2007. Lipids of marine Archaea: Patterns and provenance in the water-column and sediments. Geochim Cosmochim Acta 71:3272–3291.

Uda I, Sugai A, Itoh YH, Itoh T. 2001. Variation in molecular species of polar lipids from thermoplasma acidophilum depends on growth temperature. Lipids 36:103–105.

Van Dover CL. 2000. The Ecology of Deep-Sea Hydrothermal Vents. Princeton, NJ: Princeton University Press.

Wakeham SG, Amann R, Freeman KH, Hopmans EC, Jørgensen BB, Putnam IF, Schouten S, Sinninghe Damsté JS, Talbot HM, Woebken D. 2007. Microbial ecology of the stratified water column of the Black Sea as revealed by a comprehensive biomarker study. Organ Geochem 38:2070–2097.

Wang D, Wu S, Dong D, Yao G, Cao Q. 2009. Seismic characteristics of quaternary mass transport deposits in Qiongdongnan Basin. Mar Geol Quatern Geol 29:69–74 (In Chinese).

Wei YL, Wang JX, Liu J, Dong L, Li L, Wang H, Wang P, Zhao MX, Zhang CL. 2011. Spatial variations in archaeal lipids of surface water and core-top sediments in the South China Sea and their implications for Paleoclimate studies. Appl Environ Microbiol 77:7479–7489.

Weijers JWH, Schouten S, Spaargaren OC, Sinninghe Damsté JS. 2006. Occurrence and distribution of tetraether membrane lipids in soils: Implications for the use of the TEX_{86} proxy and the BIT index. Organ Geochem 37:1680–1693.

Wuchter C, Schouten S, Wakeham SG, Sinninghe Damsté JS. 2006. Archaeal tetraether membrane lipid fluxes in the northeastern Pacific and the Arabian Sea: Implications for TEX_{86} paleothermometry. Paleoceanography 21:PA4208.

Xie XN, Muller RD, Li ST, Gong ZS, Steinberger B. 2006. Origin of anomalous subsidence along the Northern South China Sea margin and its relationship to dynamic topography. Mar Petrol Geol 23:745–765.

Yamamoto M, Shimamoto A, Fukuhara T, Tanaka Y, Ishizaka J. 2012. Glycerol dialkyl glycerol tetraethers and TEX_{86} index in sinking particles in the western North Pacific. Organ Geochem 53: 52–62.

Yang T, Jiang SY, Ge L, Yang JH, Wu NY, Zhang GX, Liu J, Chen DH. 2013. Geochemistry of pore waters from HQ-1PC of the Qiongdongnan Basin, northern South China Sea, and its implications for gas hydrate exploration. Science China Earth Sciences: 1–9.

Zhang J, Bai Y, Xu SD, Lei F, Jia GD. 2013. Alkenone and tetraether lipids reflect different seasonal seawater temperatures in the coastal northern South China Sea. Organ Geochem 58: 115–120.

Zhang YG, Zhang CL, Liu XL, Li L, Hinrichs KU, Noakes JE. 2011. Methane Index: A tetraether archaeal lipid biomarker indicator for detecting the instability of marine gas hydrates. Earth Planet Sci Lett 307:525–534.

Zhao MX, Huang C-Y, Wang C-C, Wei GJ. 2006. A millennial-scale $U_{37}^{K'}$ sea-surface temperature record from the South China Sea (8°) over the last 150 kyr: Monsoon and sea-level influence. Palaeogeogr Palaeoclimatol Palaeoecoll 236:39–55.

Zhu C, Weijers JWH, Wagner T, Pan JM, Chen JF, Pancost RD. 2011. Sources and distributions of tetraether lipids in surface sediments across a large river-dominated continental margin. Organ Geochem 42:376–386.